

DO-TH 97/09

May 1997

Leading log radiative corrections to deep inelastic production of heavy quarks

I. Schienbein

Institut für Physik, Universität Dortmund
D-44221 Dortmund, Germany

Abstract

$\mathcal{O}(\alpha)$ QED radiative corrections to neutral current deep inelastic production of heavy quarks are calculated in the leading log approximation and compared with the corresponding corrections assuming a massless charm parton. Besides the inclusive case, corrections to the semi-inclusive $d^3\sigma/dxdydz$ and the effect of z -cuts are studied. In the latter case, the massless corrections differ from the correct massive radiative corrections to deep inelastic heavy quark production by about 40%–10% for $0.2 \lesssim z \lesssim 0.5$.

1 Introduction

Deep inelastic production of heavy quarks at HERA is important for several reasons:

- At small x ($x \approx 10^{-3}$) the charm contribution F_2^c to F_2^{ep} amounts to 20%–30% [1] making a reliable theoretical treatment of F_2^c necessary for a precision measurement of F_2^{ep} .
- The bulk of heavy quarks is produced via the photon gluon fusion mechanism [1, 2] providing the possibility to constrain the gluon distribution $g(y, \mu^2)$ in the proton [3, 4, 5].
- By measuring differential distributions, the charm production mechanism can be tested, and it can be studied whether and when the charm quark behaves like a massless parton [4, 5].

In order to estimate radiative corrections to heavy quark production, we employ the well-known leading log approximation (LLA) [6, 7, 8, 9]. See also ref. [10] where radiative corrections to heavy flavour production have been studied in the Weizsäcker-Williams approximation (WWA) using hadronic variables. The $\mathcal{O}(\alpha)$ (QED-)corrections to the process $e + g \rightarrow e + c + \bar{c}$ are shown in fig. 1 (not shown are crossed and virtual diagrams). The main part of the corrections comes from bremsstrahlung from the electron line (plus corresponding virtual corrections), see a) and b). These two contributions are enhanced by a large collinear logarithm $L_e = \ln(Q^2/m_e^2)$. In the same way, calculating c), d), and e), one gets logarithms $L_c = \ln(Q^2/m_c^2)$ which are much smaller than L_e because of the large charm mass m_c , compared to the electron mass m_e . For example, for $Q^2 = 10 \text{ GeV}^2$, one finds $L_e \approx 17.5 \gg L_c \approx 1.5$ ($m_c = 1.5 \text{ GeV}$). Diagrams d) and e) do not contribute for another reason: the photons are not resolved from the final state jets in general. (Only a light intermediary quark in diagram c) could give rise for a collinear singularity, which would have to be handled the same way as the corresponding collinear gluon emission,

leading to a negligible (at least in LLA) modification of the parton distributions.) Thus, we only take the leptonic corrections a) and b) (in $\mathcal{O}(\alpha)$ -LLA) into consideration.

The paper is organized as follows: In Sect. 2 the formulae needed to calculate radiative corrections to neutral current heavy quark production in $\mathcal{O}(\alpha)$ -LLA are collected. In Sect. 3 numerical results are presented. Finally, the main results are briefly summarized in Sect. 4.

2 Formalism

We calculate the $\mathcal{O}(\alpha)$ QED-corrections to deep inelastic production of heavy quarks in leading log approximation (LLA) [7, 8]. Following the formalism of ref. [7], the cross section for deep inelastic production of charm quarks via the photon gluon fusion (PGF) mechanism ($e + g \rightarrow e + c + \bar{c}$) reads:

$$d\sigma(ep \rightarrow ec\bar{c}X) = \int_0^1 dz_1 \int_0^1 dz_2 \int_0^1 dz_3 D_{e/e}(z_1, Q^2) g(z_2, \mu^2) \bar{D}_{e/e}(z_3, Q^2) d\hat{\sigma}(e+g \rightarrow e+c+\bar{c}) . \quad (1)$$

The functions $D_{e/e}$, $\bar{D}_{e/e}$ contain the factorized mass singularities from the electron line and are, up to $\mathcal{O}(\alpha)$, given by [7]

$$D_{e/e}(x, Q^2) = \bar{D}_{e/e}(x, Q^2) = \delta(1-x) + \left(\frac{\alpha L_e}{2\pi} \right) P_{ee}(x) \quad (2)$$

with

$$L_e \equiv \ln \frac{Q^2}{m_e^2} \quad (3)$$

and the splitting function

$$P_{ee}(x) = \left[\frac{1+x^2}{1-x} \right]_+ = \frac{1+x^2}{(1-x)_+} + \frac{3}{2} \delta(1-x). \quad (4)$$

The (+)-distribution is defined by

$$\int_x^1 dz P_{ee}(z) f(z) = \int_x^1 dz \frac{1+z^2}{1-z} (f(z) - f(1)) - \int_0^x dz \frac{1+z^2}{1-z} f(1) . \quad (5)$$

$D_{e/e}(z_1, Q^2)$ can be interpreted as the probability of finding an electron with momentum fraction z_1 inside the incoming electron, $\bar{D}_{e/e}(z_3, Q^2)$ describes the fragmentation of the scattered electron into the observed outgoing electron with momentum fraction z_3 , and $g(z_2, \mu^2)$ is the gluon density inside the proton. Finally, $d\hat{\sigma}$ is the cross section of the underlying hard scattering subprocess.

The variables x , y and Q^2 are reconstructed by the 4-momentum p'_e of the observed electron and the 4-momenta p_e , p of the initial state electron and proton:

$$q_l \equiv p_e - p'_e, \quad Q_l^2 \equiv -q_l^2, \quad y_l = \frac{p \cdot q_l}{p \cdot p_e}, \quad x_l \equiv \frac{Q_l^2}{2p \cdot q_l} = \frac{Q_l^2}{S y_l}, \quad (6)$$

where $S \equiv (p + p_e)^2$. In the same way, one defines for the hard scattering process $e(\hat{p}_e = z_1 p_e) + g(\hat{p} = z_2 p) \longrightarrow e(\hat{p}'_e = p'_e/z_3) + c(p_c) + X$:

$$\hat{q} = \hat{p}_e - \hat{p}'_e, \quad \hat{Q}^2 = -\hat{q}^2 = \frac{z_1}{z_3} Q_l^2, \quad \hat{y} = \frac{\hat{p} \hat{q}}{\hat{p} \hat{p}_e} = \frac{z_1 z_3 - 1 + y_l}{z_1 z_3}, \quad (7)$$

$$\hat{x} = \frac{\hat{Q}^2}{2\hat{p} \cdot \hat{q}} = \frac{\hat{Q}^2}{\hat{S} \hat{y}} = \frac{z_1 x_l y_l}{z_2 (z_1 z_3 - 1 + y_l)}, \quad \hat{S} = (\hat{p}_e + \hat{p})^2 = z_1 z_2 S. \quad (8)$$

Because we only use leptonic variables x_l , y_l , etc. , the index l will be suppressed from now on.

In the following, we calculate the radiative corrections to the photon gluon fusion (PGF) subprocess

$$e(\hat{p}_e) + g(\hat{p}) \longrightarrow e(\hat{p}'_e) + c(p_c) + \bar{c}(p_{\bar{c}}). \quad (9)$$

and compare the results with the radiative corrections to the charm excitation (CE) subprocess

$$e(\hat{p}_e) + c(\hat{p}) \longrightarrow e(\hat{p}'_e) + c(p_c) \quad (10)$$

where, in contrast to the PGF, the charm quark is treated as an intrinsic (massless) parton of the proton. The latter process has been used by the H1 Collab. [11] in a recent analysis of leptonproduction of D-mesons [1], employing some charm density $c(x, \mu^2)$.

2.1 Inclusive case

2.1.1 Photon gluon fusion (PGF)

The hard cross section for the process (9) can be written as:

$$\frac{d^2\hat{\sigma}}{d\hat{x}d\hat{y}} = \frac{4\pi\alpha^2\hat{S}}{\hat{Q}^4} \left[(1-\hat{y})f_2(\hat{x}, \hat{Q}^2) + \hat{x}\hat{y}^2f_1(\hat{x}, \hat{Q}^2) \right] \quad (11)$$

with the partonic structure functions [12, 13, 14, 15]

$$f_k(\hat{x}, \hat{Q}^2, m_c^2, \mu^2) = \frac{\alpha_s(\mu^2)}{\pi} \frac{\hat{\xi}}{4\pi} e_c^2 c_{k,g}^{(0)}(\hat{x}, \hat{Q}^2) \theta(\hat{W}^2 - 4m_c^2), \quad k = 2, L, \quad (12)$$

$$f_1(\hat{x}, \hat{Q}^2, m_c^2, \mu^2) = \frac{1}{2\hat{x}}(f_2 - f_L), \quad (13)$$

$$\begin{aligned} \frac{\hat{\xi}}{4\pi} c_{2,g}^{(0)} &= \left[\frac{\hat{x}}{2} - \hat{x}^2(1-\hat{x}) + 2\frac{m_c^2}{\hat{Q}^2}\hat{x}^2(1-3\hat{x}) - 4\frac{m_c^4}{\hat{Q}^4}\hat{x}^3 \right] \ln \frac{1+\hat{\beta}}{1-\hat{\beta}} \\ &\quad + \hat{\beta} \left[4\hat{x}^2(1-\hat{x}) - \frac{\hat{x}}{2} - 2\frac{m_c^2}{\hat{Q}^2}\hat{x}^2(1-\hat{x}) \right], \end{aligned} \quad (14)$$

$$\frac{\hat{\xi}}{4\pi} c_{L,g}^{(0)} = -4\frac{m_c^2}{\hat{Q}^2}\hat{x}^3 \ln \frac{1+\hat{\beta}}{1-\hat{\beta}} + 2\hat{\beta}\hat{x}^2(1-\hat{x}), \quad (15)$$

where e_c , m_c are the charm quark charge and mass, respectively, $\hat{\xi} \equiv \xi(\hat{Q}^2) = \frac{\hat{Q}^2}{m_c^2}$, $\hat{W}^2 \equiv W^2(\hat{x}, \hat{Q}^2) = \frac{\hat{Q}^2(1-\hat{x})}{\hat{x}}$, and $\hat{\beta}^2 \equiv \beta^2(\hat{x}, \hat{Q}^2) = 1 - 4m_c^2/\hat{W}^2$.

By insertion of eq. (2), (11) into eq. (1), one obtains the cross section $d\sigma = d\sigma^0 + d\sigma^i + d\sigma^f$. The Born cross section $d\sigma^0$ is given by

$$\frac{d^2\sigma^0}{dx dy} = \frac{4\pi\alpha^2 S}{Q^4} \left[(1-y)F_2(x, Q^2) + xy^2F_1(x, Q^2) \right] \quad (16)$$

with the leading order structure functions

$$F_1(x, Q^2, \mu^2, m_c^2) = \int_{ax}^1 \frac{dz_2}{z_2} g(z_2, \mu^2) f_1(x/z_2, Q^2, m_c^2, \mu^2), \quad (17)$$

$$F_2(x, Q^2, \mu^2, m_c^2) = \int_{ax}^1 \frac{dz_2}{z_2} z_2 g(z_2, \mu^2) f_2(x/z_2, Q^2, m_c^2, \mu^2), \quad (18)$$

where $a = 1 + 4m_c^2/Q^2$. $d\sigma^{i,f}$ contain the contribution due to radiation of a collinear photon from the incoming (initial state radiation, ISR) and outgoing electron (final state

radiation, FSR), respectively:

$$\begin{aligned} \frac{d^2\sigma^i}{dxdy} &= \frac{\alpha L_e}{2\pi} \int_{z_1^{min}}^1 dz_1 \left[\frac{1+z_1^2}{1-z_1} (\sigma_0(z_1, 1) - \sigma_0(1, 1)) \right] \\ &+ \frac{\alpha L_e}{2\pi} H(z_1^{min}) \sigma_0(1, 1), \end{aligned} \quad (19)$$

$$\begin{aligned} \frac{d^2\sigma^f}{dxdy} &= \frac{\alpha L_e}{2\pi} \int_{z_3^{min}}^1 dz_3 \left[\frac{1+z_3^2}{1-z_3} (\sigma_0(1, z_3) - \sigma_0(1, 1)) \right] \\ &+ \frac{\alpha L_e}{2\pi} H(z_3^{min}) \sigma_0(1, 1), \end{aligned} \quad (20)$$

with

$$\sigma_0(z_1, z_3) = \int_{z_2^{min}}^1 dz_2 g(z_2, \mu^2) \frac{\partial(\hat{x}, \hat{y})}{\partial(x, y)} \frac{d^2\hat{\sigma}}{d\hat{x}d\hat{y}}, \quad (21)$$

$$H(z) = - \int_0^z dx \frac{1+x^2}{1-x} = 2 \ln(1-z) + z + \frac{1}{2}z^2, \quad (22)$$

and the Jacobian

$$\frac{\partial(\hat{x}, \hat{y})}{\partial(x, y)} = \frac{y}{z_2 z_3 (z_1 z_3 - 1 + y)}. \quad (23)$$

The electromagnetic coupling is taken to be $\alpha \equiv \alpha(Q^2 = m_e^2) = 1/137.036^1$. The integration bounds

$$\begin{aligned} z_1^{min} &= \frac{1-y}{1-xy} + \frac{4m_c^2}{S(1-xy)}, \\ z_3^{min} &= \frac{1-y+xy}{1-4m_c^2/S}, \\ z_2^{min}(z_1, z_3) &= \left(1 + \frac{4m_c^2}{Q^2} \frac{z_3}{z_1} \right) z_1 xy \frac{1}{z_1 z_3 + y - 1} \end{aligned} \quad (24)$$

follow from the conditions $\hat{W}^2 \geq 4m_c^2$, $0 \leq z_2^{min}(z_1, z_3) \leq 1$. If no photon is radiated ($z_1 = 1, z_3 = 1$), one finds the well-known expression $z_2^{min}(1, 1) = (1 + 4m_c^2/Q^2)x \equiv ax$. In the kinematical region of small x , the bounds read approximately: $z_1^{min} = z_3^{min} = 1 - y + \mathcal{O}(x) + \mathcal{O}(m_c^2/S)$. It should be remarked that σ_0 is related to the Born cross section by $d^2\sigma^0/dxdy = \sigma_0(1, 1)$.

¹ Using a running coupling $\alpha(Q^2)$ according to eq. (14) in [7], taking effective quark masses [16] $m_u = m_d = 0.041$, $m_s = .15$, $m_c = 1.5$, and $m_b = 4.5$ GeV, instead of a constant α , leads to negligible differences.

2.1.2 Charm excitation (CE)

In the case of electron quark scattering, the radiative corrections in LLA are known up to $\mathcal{O}(\alpha^2)$ [6, 7, 8, 9, 16]. For comparison with eq. (19), (20), we use equations (22)–(29) in [7], with the charm quark as the only massless parton (MP) in the initial state. Furthermore, contributions due to Z -exchange can be neglected in the realm of $Q^2 \leq 50 \text{ GeV}^2$, i. e. , we make the replacements $A^c \rightarrow e_c^2$, $B^c \rightarrow 0$ (in eq. (22)–(29) in [7]). For the partonic structure functions, the simple relations

$$f_2(\hat{x}, \hat{Q}^2) = e_c^2 \delta(1 - \hat{x}) , \quad (25)$$

$$f_1(\hat{x}, \hat{Q}^2) = \frac{1}{2\hat{x}} f_2(\hat{x}, \hat{Q}^2) \quad (26)$$

hold, and one easily finds [7]

$$\sigma_0(z_1, z_3) = \frac{2\pi\alpha^2 y}{z_1 z_3^2 \hat{y}^3 \hat{S}} [1 + (1 - \hat{y})^2] e_c^2 \left(c(\bar{z}_2, \hat{Q}^2) + \bar{c}(\bar{z}_2, \hat{Q}^2) \right) \quad (27)$$

with

$$\bar{z}_2 = \frac{z_1 x y}{z_1 z_3 + y - 1} , \quad z_1^{min} = \frac{1 - y}{1 - x y} , \quad z_3^{min} = 1 - y(1 - x) . \quad (28)$$

(Of course, eq. (27) and (28) have to be inserted into eq. (19) and (20).)

Finally, we briefly discuss the Compton contribution $d\sigma^C$ to the radiative corrections which can be obtained from eq. (21) ($Q_0 = 200 \text{ MeV}$) and (29) in [7], only allowing for the charm (or anti-charm) quark in the initial state. Fig. 2 displays the Compton contribution $\delta^C = \frac{d^2\sigma^C}{dx dy} / \frac{d^2\sigma^0}{dx dy}$ for $x = 10^{-2}$ (dashed line) and $x = 10^{-3}$ (full line) using the CTEQ4L parton distributions [17]. For $y \lesssim 0.7$, δ^C is small and can be safely neglected for experimentally relevant values of y [1].

2.2 z -differential case

In order to calculate radiative corrections to the z -differential cross section $d^3\sigma^D/dx dy dz$, where $z = p \cdot p_D / p \cdot q$, the fragmentation of the charm quark into the observed D -meson

must be taken into consideration. Thus, it is necessary to extend eq. (1):

$$d\sigma(ep \rightarrow eDX) = \int_0^1 dz_1 \int_0^1 dz_2 \int_0^1 dz_3 D_{e/e}(z_1, Q^2) g(z_2, \mu^2) \bar{D}_{e/e}(z_3, Q^2) \int_0^1 dz_4 D_c(z_4) d\hat{\sigma}. \quad (29)$$

The hadronization of the outgoing charm quark with momentum p_c into the observed D -meson with momentum $p_D = z_4 p_c$ is modeled by the fragmentation function $D_c(z_4)$. Writing the partonic cross section differential in $\hat{z}_c = \hat{p} \cdot p_c / \hat{p} \cdot \hat{q}$, the relations in eq. (7) have to be accomplished with

$$\hat{z}_c = \frac{zyz_3}{z_4(z_1 z_3 + y - 1)} \equiv \frac{z}{z_4} r, \quad (30)$$

with r defined by

$$r \equiv \frac{y z_3}{z_1 z_3 + y - 1}, \quad (31)$$

which can be derived from the definitions of \hat{z}_c , z and \hat{q} , using $p_D = z_4 p_c$.

In analogy to the above discussion, we compare the “massive” (PGF) with the “massless” (CE) corrections, using a massless charm parton (MP).

2.2.1 Photon gluon fusion

The partonic cross section reads

$$\frac{d^3 \hat{\sigma}}{d\hat{x} d\hat{y} d\hat{z}_c} = \frac{4\pi\alpha^2 \hat{S}}{\hat{Q}^4} \left[(1 - \hat{y}) f_2(\hat{x}, \hat{Q}^2; \hat{z}_c) + \hat{x} \hat{y}^2 f_1(\hat{x}, \hat{Q}^2; \hat{z}_c) \right], \quad (32)$$

where the structure functions are given by ²

$$f_2(x, Q^2; \zeta) = \frac{\alpha_s}{\pi} e_c^2 x \left[\frac{1}{4} \text{BG}(x, Q^2, \zeta, m_c) + \frac{3}{4} \text{BL}(x, Q^2, \zeta, m_c) \right], \quad (33)$$

$$f_L(x, Q^2; \zeta) = \frac{\alpha_s}{\pi} e_c^2 x \frac{1}{2} \text{BL}(x, Q^2, \zeta, m_c), \quad (34)$$

with

$$\text{BL}(x, Q^2, \zeta, m_c) = 4x \left[1 - x - x \frac{m_c^2}{Q^2} \frac{1}{\zeta(1 - \zeta)} \right],$$

²The corresponding expressions for general boson gluon fusion can be found in [19].

$$\begin{aligned} \text{BG}(x, Q^2, \zeta, m_c) &= -2 + \left[1 - 2x + 2x^2 + 4\frac{m_c^2}{Q^2}x(1-x) \right] \frac{1}{\zeta(1-\zeta)} \\ &\quad + 2x^2\frac{m_c^2}{Q^2} \left(1 - 2\frac{m_c^2}{Q^2} \right) \frac{1}{(1-\zeta)^2\zeta^2}, \end{aligned}$$

$$[15, 18] \text{ and } f_1(\hat{x}, \hat{Q}^2; \hat{z}_c) = \frac{1}{2\hat{x}} \left[f_2(\hat{x}, \hat{Q}^2; \hat{z}_c) - f_L(\hat{x}, \hat{Q}^2; \hat{z}_c) \right].$$

The cross sections for ISR and FSR have the same structure as in eq. (19) and (20) with a z dependent function σ_0 :

$$\begin{aligned} \frac{d^3\sigma^i}{dxdydz} &= \frac{\alpha L_e}{2\pi} \int_{z_1^{\min}}^1 dz_1 \left[\frac{1+z_1^2}{1-z_1} (\sigma_0(z_1, 1; z) - \sigma_0(1, 1; z)) \right] \\ &\quad + \frac{\alpha L_e}{2\pi} H(z_1^{\min}) \sigma_0(1, 1; z), \end{aligned} \quad (35)$$

$$\begin{aligned} \frac{d^3\sigma^f}{dxdydz} &= \frac{\alpha L_e}{2\pi} \int_{z_3^{\min}}^1 dz_3 \left[\frac{1+z_3^2}{1-z_3} (\sigma_0(1, z_3; z) - \sigma_0(1, 1; z)) \right] \\ &\quad + \frac{\alpha L_e}{2\pi} H(z_3^{\min}) \sigma_0(1, 1; z), \end{aligned} \quad (36)$$

with

$$\sigma_0(z_1, z_3; z) = \int_{z_2^{\min}}^1 dz_2 g(z_2, \mu^2) \int_{z_4^{\min}}^{z_4^{\max}} dz_4 \frac{\partial(\hat{x}, \hat{y}, \hat{z}_c)}{\partial(x, y, z)} \frac{d^3\hat{\sigma}}{d\hat{x}d\hat{y}d\hat{z}_c} D_c(z_4). \quad (37)$$

The Jacobian in eq. (37) can easily be calculated as

$$\frac{\partial(\hat{x}, \hat{y}, \hat{z}_c)}{\partial(x, y, z)} = \frac{\partial(\hat{x}, \hat{y})}{\partial(x, y)} \frac{\partial\hat{z}_c}{\partial z} = \frac{y^2}{z_2 z_4 (z_1 z_3 - 1 + y)^2}. \quad (38)$$

The integration bounds can be derived from the conditions $\hat{W}^2 = \frac{\hat{Q}^2(1-\hat{x})}{\hat{x}} \geq 4m_c^2$, leading to eq. (24), and $\hat{z}_c^{\min} \leq \hat{z}_c \leq \hat{z}_c^{\max}$ with $\hat{z}_c^{\min} = \frac{1 \pm \beta(\hat{x}, \hat{Q}^2)}{2}$ [18], where $\beta^2(\hat{x}, \hat{Q}^2) = 1 - 4m_c^2/\hat{W}^2$, implying

$$z_4^{\max} = \min \left[1, \frac{zr}{\hat{z}_c^{\min}} \right], \quad (39)$$

$$z_4^{\min} = \min \left[z_4^{\max}, \frac{zr}{\hat{z}_c^{\max}} \right] \quad (40)$$

with r from eq. (31). For $D_c(z)$, we use a Peterson et al. fragmentation function [20]

$$D_c(z) = N \left\{ z \left[1 - z^{-1} - \varepsilon_c/(1-z) \right]^2 \right\}^{-1}, \quad (41)$$

normalized to $\int_0^1 dz D_c(z) = 1$, i. e. ,

$$N^{-1} = \frac{(\varepsilon_c^2 - 6\varepsilon_c + 4)}{(4 - \varepsilon_c)\sqrt{4\varepsilon_c - \varepsilon_c^2}} \left\{ \arctan \frac{\varepsilon_c}{\sqrt{4\varepsilon_c - \varepsilon_c^2}} + \arctan \frac{2 - \varepsilon_c}{\sqrt{4\varepsilon_c - \varepsilon_c^2}} \right\} + \frac{1}{2} \ln \varepsilon_c + \frac{1}{4 - \varepsilon_c} . \quad (42)$$

2.2.2 Flavor excitation

In the subprocess $e + c \longrightarrow e + c$ we have $\hat{z}_c = \hat{p} \cdot p_c / \hat{p} \cdot \hat{q} = 1$, following from $p_c = \hat{q} + \hat{p}$. Thus, one obtains the \hat{z}_c -differential cross section by inserting the structure functions

$$f_2(\hat{x}, \hat{Q}^2, \hat{z}_c) = e_c^2 \delta(1 - \hat{x}) \delta(1 - \hat{z}_c) \quad (43)$$

$$f_1(\hat{x}, \hat{Q}^2, \hat{z}_c) = \frac{1}{2\hat{x}} f_2(\hat{x}, \hat{Q}^2, \hat{z}_c) \quad (44)$$

into eq. (11). Because of $\delta(1 - \hat{z}_c) = z_4 \delta(z_4 - rz)$ and $\partial \hat{z}_c / \partial z = r/z_4$ one finds

$$\sigma_0(z_1, z_3; z) = \sigma_0(z_1, z_3) r D_c(rz) \quad (45)$$

with $\sigma_0(z_1, z_3)$ from eq. (27) and r from eq. (31).

Finally the z -differential corrections are given by eq. (35) and (36) with σ_0 from eq. (45) and the integration bounds

$$z_1^{min} = \max \left[\frac{1-y}{1-xy}, 1-y(1-z) \right], \quad (46)$$

$$z_3^{min} = \max \left[1-y(1-x), \frac{1-y}{1-yz} \right]. \quad (47)$$

The second boundary in $\max[\dots]$ can be deduced from $0 \leq rz \leq 1$.

Eq. (35), (36) can easily be tested:

$$\int_0^1 dz \frac{d^3 \sigma^{i,f}}{dx dy dz} \stackrel{!}{=} \frac{d^2 \sigma^{i,f}}{dx dy}, \quad (48)$$

with $d^2 \sigma^{i,f}/dx dy$ from (19), (20). The Compton contribution will be neglected for the same reasons as in the inclusive case.

3 Numerical results

As usual, the radiative corrections will be shown in form of a correction factor δ defined by $d\sigma = d\sigma^0(1 + \delta)$, i. e., $\delta = \delta^i + \delta^f + \dots$ with

$$\delta^{i,f}(x, y) = \frac{d^2\sigma^{i,f}}{dxdy} / \frac{d^2\sigma^0}{dxdy}$$

or, in the z -differential case,

$$\delta^{i,f}(x, y, z) = \frac{d^3\sigma^{i,f}}{dxdydz} / \frac{d^3\sigma^0}{dxdydz}.$$

In all figures we use HERA centre-of-mass energies $S = 4 \cdot 27.5 \cdot 820 \text{ GeV}^2$.

Fig. 3 shows the radiative corrections to heavy quark production (PGF) for experimentally relevant values³ of Bjorken- x [1] as a function of y according to eq. (19) and (20) using the GRV94(LO) parton distributions [21]. The factorization scale has been chosen to be $\mu^2 = Q^2 + 4m_c^2$ [3] with $m_c = 1.5 \text{ GeV}$. For $x = 10^{-2}$, the typical shape of radiative corrections in leptonic variables can be seen, with large corrections for $y \rightarrow 1$, whereas for smaller $x \leq 10^{-3}$ the curves become more and more flat for $y \rightarrow 1$.

The theoretical uncertainties due to different choices of parton distributions, factorization scales, and charm masses turn out to be small, as can be seen in fig. 4 and fig. 5. One finds $\delta(\text{CTEQ}) - \delta(\text{GRV}) < 0.02$, $\delta(m_c = 1.3) - \delta(m_c = 1.7) < 0.03$ for relevant $y \leq 0.7$, and $\delta(\mu^2 = 4m_c^2) - \delta(\mu^2 = Q^2 + 4m_c^2) < 0.03$, where the scale $\mu^2 = 4m_c^2$ has been favored in [22]. This could be expected because variations of μ , m_c , or the parton distributions lead to rather similar changes in $d\sigma^0$ and $d\sigma^{i,f}$, so that the quotient δ does not change too much.

In the recent analysis of deep inelastic charm production by the H1 Collab. [1], the radiative corrections have been calculated in $\mathcal{O}(\alpha)$ -LLA with the HECTOR package [16] using the charm excitation subprocess ($F_L^c = 0$) and the GRV92 parton distributions [23]. Furthermore, only initial state radiation has been taken into consideration, assuming the

³For a clean extraction of the gluon density it is necessary to extend the x -range to $x \lesssim 5 \cdot 10^{-4}$ [5].

collinear final state photon not to be separated from the outgoing electron [11], leading to small corrections. Because PGF has been measured to be the dominant ($> 95\%$) charm production mechanism in the small x (and Q^2) range [1], it is necessary to check if the “massless” corrections (δ^{MP}) agree with the “massive” ones (δ^{PGF}). In fig. 6 we compare the massive ($\mu^2 = Q^2 + 4m_c^2$; $m_c = 1.5$ GeV) with the massless corrections due to initial state radiation. The experimentally relevant values of Q^2 [1] are indicated by dotted vertical lines. The conversion of “masslessly corrected” (δ^{MP}) data to “massively corrected” (δ^{PGF}) data can be performed by applying the factor $R \equiv (1 + \delta^{MP})/(1 + \delta^{PGF})$ because of

$$\begin{aligned} d\sigma(\text{PGF}) &= d\sigma(\text{exp}) \frac{1}{1 + \delta^{\text{PGF}}} \\ &= d\sigma(\text{MP}) \frac{1 + \delta^{\text{MP}}}{1 + \delta^{\text{PGF}}} \equiv d\sigma(\text{MP}) R . \end{aligned}$$

For the (x, Q^2) data points one finds $|R - 1| = |\delta^{MP} - \delta^{PGF}|/(1 + \delta^{PGF}) < 3\%$, i. e. , the differences between massless and massive radiative corrections lead to a small increase ($\delta^{MP} > \delta^{PGF}$) of the data. However, this difference is small enough to use the simpler charm excitation subprocess for calculating the radiative corrections in the inclusive case.

Of course, heavy quark production processes are exclusive in the heavy quark momentum and on this more differential level the photon gluon fusion and the charm excitation processes are not compatible which can be seen, e.g., from the different shapes of the $x_D = |\vec{p}_D^*|/|\vec{p}_p^*| = 2|\vec{p}_D^*|/W$ distributions shown in the experimental analyses [1, 2] (fig. 6, fig. 1 resp.). We prefer to employ the lorentz-invariant variable $z = p \cdot p_D / p \cdot q$ which approximately transforms into x_D in the γ^*-p centre-of-mass system, following the argumentation in [1]. This can be easily seen by calculating z in the γ^*-p -CMS. One finds $z = x_D \sin^2 \theta^* / 2$ with⁴ $\theta^* = \angle(\vec{p}_p^*, \vec{p}_D^*) \approx \pi$.

In fig. 7 we show the z -differential radiative corrections according to eq. (35), (36), (37) (PGF, full line) and (45) (MP, dashed line), where it has been integrated over the

⁴ $\vec{p}_\gamma^* + \vec{p}_p^* = 0$, $\vec{p}_{g,c}^* = z_2 \vec{p}_p^* \Rightarrow \vec{p}_\gamma^* + \vec{p}_{g,c}^* = -(1 - z_2) \vec{p}_p^*$. This means for the CE-subprocess: $\vec{p}_\gamma^* + \vec{p}_c^* = \vec{p}_c^* = z_4 \vec{p}_D^* \Rightarrow \theta^* = \pi$ and for the PGF: $\vec{p}_\gamma^* + \vec{p}_g^* = \vec{p}_c^* + \vec{p}_e^* \Rightarrow \theta^* \approx \pi$ (the collinear configuration is dominant). Note that an angle $\theta^* = 160^\circ$ still yields $\sin^2 \theta^* / 2 = 0.97$.

kinematical range $10 \text{ GeV}^2 \leq Q^2 \leq 100 \text{ GeV}^2$, $0.01 \leq y \leq 0.7$. The left hand side shows the correction factor $\delta^i = d\sigma^i/d\sigma^0$ as well as the sum of initial and final state radiation $\delta^i + \delta^f$. In all cases, we employed the GRV92(LO) (massless) [23] and GRV94(LO) (massive) [21] parton distributions, in the massive case with $m_c = 1.5 \text{ GeV}$ and $\mu^2 = Q^2 + 4m_c^2$. For D_c a Peterson et al. fragmentation function [20] with $\varepsilon = 0.15$ has been taken. To study the dependence of δ on ε , we compare the radiative corrections for two different choices of ε in fig. 8. In the massive case the ε -dependence is obviously small, whereas for massless corrections one finds big differences in the steep region $z \lesssim 0.4$. Fig. 7 reveals a rather big difference between massive and massless corrections for $z \lesssim 0.5$. For $z \rightarrow 1$ only soft photon radiation is allowed, so that the corrections factorize and become independent of the underlying subprocess. On this more differential level it is necessary to calculate the radiative corrections using the photon gluon fusion subprocess because of the big deviations of the massless from the massive corrections for $z \lesssim 0.5$. On the right side of fig. 7 the z -dependence of the cross sections $d\sigma^{0,i,f}$ is displayed. Integration over $0 \leq z \leq 1$ leads to the observed small differences between massless and massive corrections because positive and negative contributions compensate each other. To get an impression of the effect of z -cuts, we show in fig. 9 the correction factor $\delta^{i,f}(x, y; z^{\min}, z^{\max}) = \int_{z^{\min}}^{z^{\max}} dz \frac{d\sigma^{i,f}}{dx dy dz} / \int_{z^{\min}}^{z^{\max}} dz \frac{d\sigma^0}{dx dy dz}$ for three z -integration ranges, from top to bottom $z^{\min} = 0 \leq z \leq z^{\max} = 1$, $0.2 \leq z \leq 0.8$, and $0.3 \leq z \leq 0.9$ for $x = 10^{-3}$. For completeness, we used the GRV94/92(LO) parton distributions [21], [23] for the massive ($m_c = 1.5 \text{ GeV}$, $\mu^2 = Q^2 + 4m_c^2$) and massless corrections and a Peterson et al. fragmentation function [20] with $\varepsilon = 0.15$. As can be seen from fig. 7, a cut $z \gtrsim 0.2$ leads to the exclusion of positive contributions of $d\sigma^{i,f}$, diminishing the radiative corrections.

4 Summary

The $\mathcal{O}(\alpha)$ -QED corrections to inclusive and z -differential deep inelastic electroproduction of heavy quarks have been calculated in the leading log approximation, using electron

variables. The results have been compared to the radiative corrections in the MP scheme, where the charm quark is assumed to be a massless parton in the proton. In the inclusive case, the differences between these two approaches turned out to be negligible. However, the measurement of heavy quark production is of course differential in the momentum of the (observed) heavy quark, recommending to perform the radiative corrections on the same differential level. Thus, we have considered the semi-inclusive z -differential case, in which the massive corrections have to be applied, i.e., using the photon gluon fusion subprocess, because for $0.2 \lesssim z \lesssim 0.5$ the massless corrections differ from the massive ones by about $\approx 40\%$ – 10% . Furthermore, we studied the effect of cuts on the z -integration range. A cut $z \gtrsim 0.2$, e.g., excludes positive contributions of $d\sigma^{i,f}$, so that the $(z^{\min} \leq z \leq z^{\max})$ -integrated corrections are smaller as in the fully inclusive, i.e., $(0 \leq z \leq 1)$ -integrated case.

Acknowledgements

We thank E. Reya and M. Glück for advice and useful discussions.

References

- [1] C. Adloff et al., H1 Collab., Z. Phys. **C72** (1996) 593.
- [2] G. Abbiendi et al., ZEUS Collab., DESY 97-089, hep-ex/9706009.
- [3] A. Vogt, DESY 96-012.
- [4] E. Laenen et al., in *Proceedings of the workshop on Future Physics at HERA*, DESY, 1996, G. Ingelman, A. D. Roeck und R. Klanner (ed.) vol. 1, p. 393.
- [5] K. Daum et al., in *Proceedings of the workshop on Future Physics at HERA*, DESY, 1996, G. Ingelman, A. D. Roeck and R. Klanner (ed.) vol. 1, p. 89.
- [6] J. Kripfganz and H.-J. Möhring, Z. Phys. **C38** (1988) 653.
- [7] J. Kripfganz, H.-J. Möhring and H. Spiesberger, Z. Phys. **C49** (1991) 501.
- [8] J. Blümlein, Z. Phys. **C47** (1990) 89.
- [9] J. Blümlein, Z. Phys. **C65** (1995) 293.
- [10] J. Blümlein, Phys. Lett. **B271** (1991) 267.
- [11] S. Glazov (private communication).
- [12] E. Witten, Nucl. Phys. **B104** (1976) 445;
J. Babcock and D. Sivers, Phys. Rev. **D18** (1978) 2301;
M. A. Shifman, A. I. Vainshtein and V. I. Zakharov, Nucl. Phys. **B136** (1978) 157.
- [13] M. Glück and E. Reya, Phys. Lett. **83B** (1979) 98.
- [14] J. P. Leveille and T. Weiler, Nucl. Phys. **B147** (1979) 147.
- [15] E. Laenen, S. Riemersma, J. Smith and W. L. van Neerven, Nucl. Phys. **B392** (1993) 162.
- [16] A. Arbuzov et al., Comp. Phys. Comm. **94** (1996) 128.

- [17] H. L. Lai et al., CTEQ Collab., Phys. Rev. **D55** (1997) 1280.
- [18] G. Schuler, Nucl. Phys. **B299** (1988) 21.
- [19] S. Kretzer and I. Schienbein, DO-TH 97/02 (Phys. Rev. **D**, to appear).
- [20] C. Peterson et al., Phys. Rev. **D27** (1983) 105.
- [21] M. Glück, E. Reya and A. Vogt, Z. Phys. **C67** (1995) 433.
- [22] M. Glück, E. Reya and M. Stratmann, Nucl. Phys. **B422** (1994) 37.
- [23] M. Glück, E. Reya and A. Vogt, Z. Phys. **C53** (1992) 127.

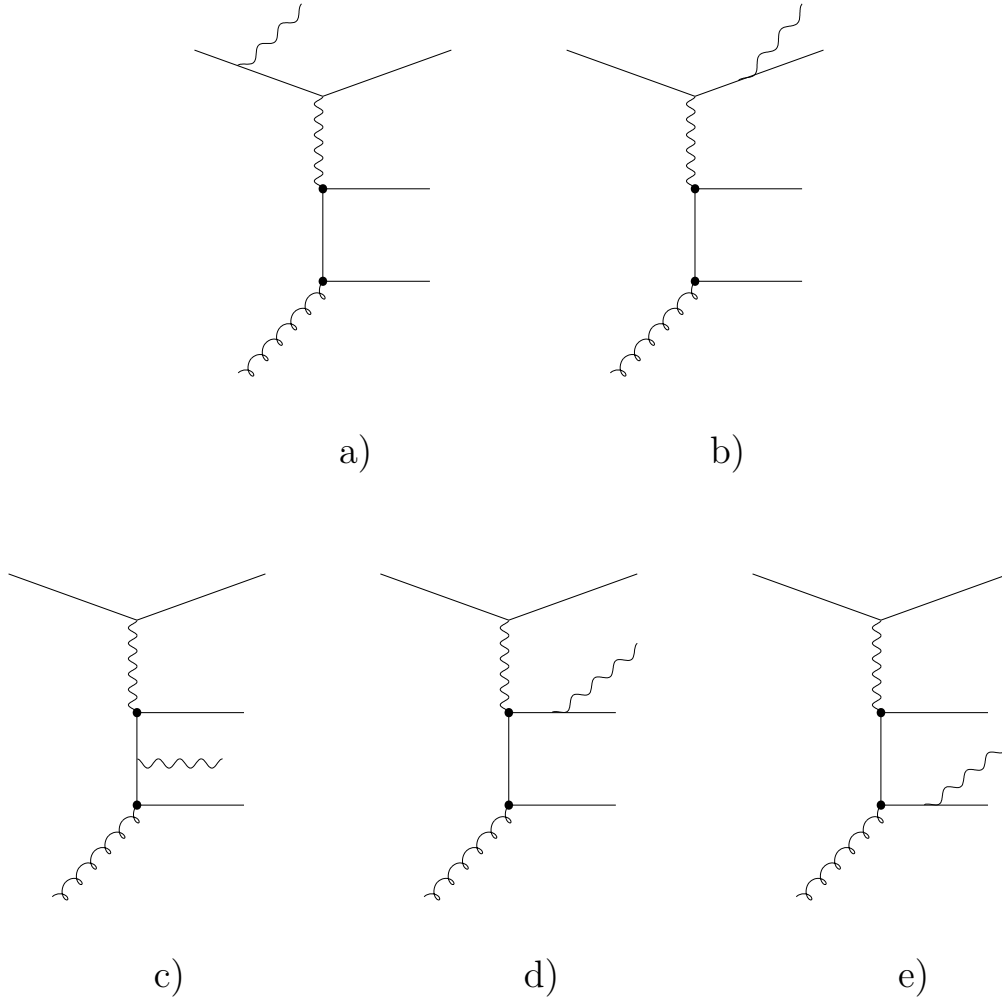


Figure 1: Real $\mathcal{O}(\alpha)$ corrections to deep inelastic production of heavy quarks via the process $e + g \rightarrow e + c + \bar{c}$. Not shown are the corresponding crossed diagrams.

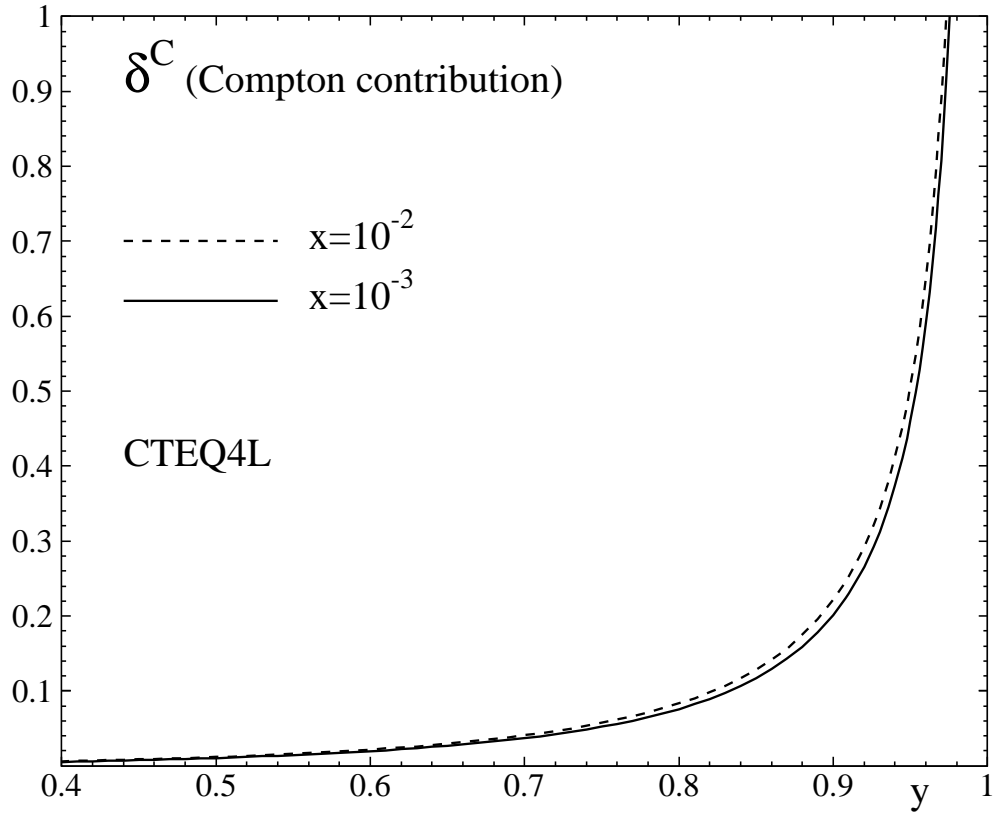


Figure 2: Compton contribution δ^C according to eq. (29) in [7] ($Q_0 = 200$ MeV, considering only the (anti-)charm quark in the initial state) with $x = 10^{-3}$ (full line) and $x = 10^{-2}$ (dashed line), employing the CTEQ4L parton densities [17].

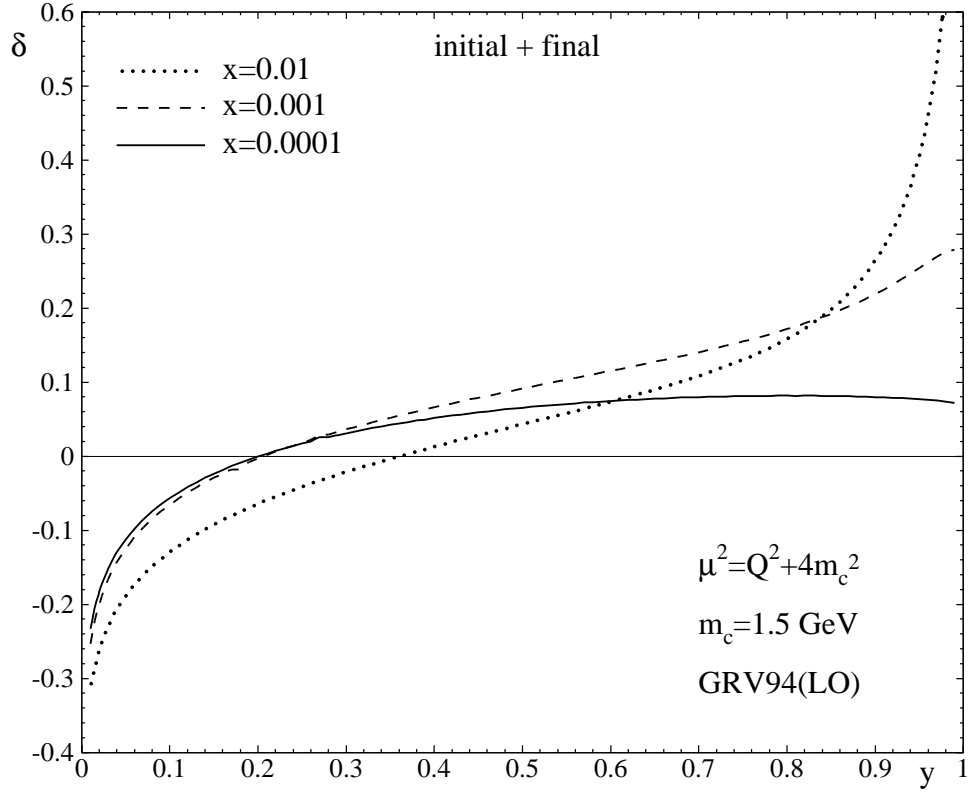


Figure 3: Radiative corrections to heavy quark production (PGF) in $\mathcal{O}(\alpha)$ -LLA, using the GRV94(LO) parton distributions [21] and the factorization scale $\mu^2 = Q^2 + 4m_c^2$ with $m_c = 1.5$ GeV. ("initial" and "final" refers to initial and final state radiation.)

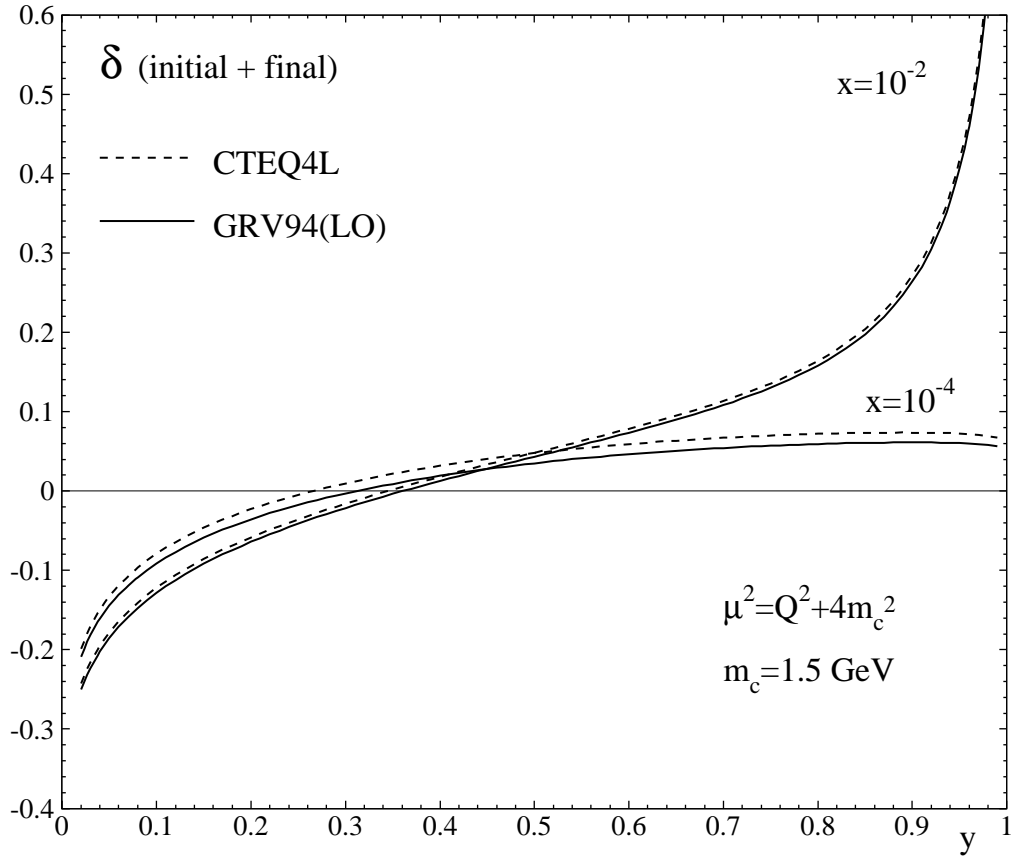


Figure 4: $\delta(x, y)$, using the GRV94(LO) [21] (full line) and CTEQ4L parton densities [17] (dashed line) with $x = 10^{-2}$ and $x = 10^{-4}$, $\mu^2 = Q^2 + 4m_c^2$ and $m_c = 1.5 \text{ GeV}$.

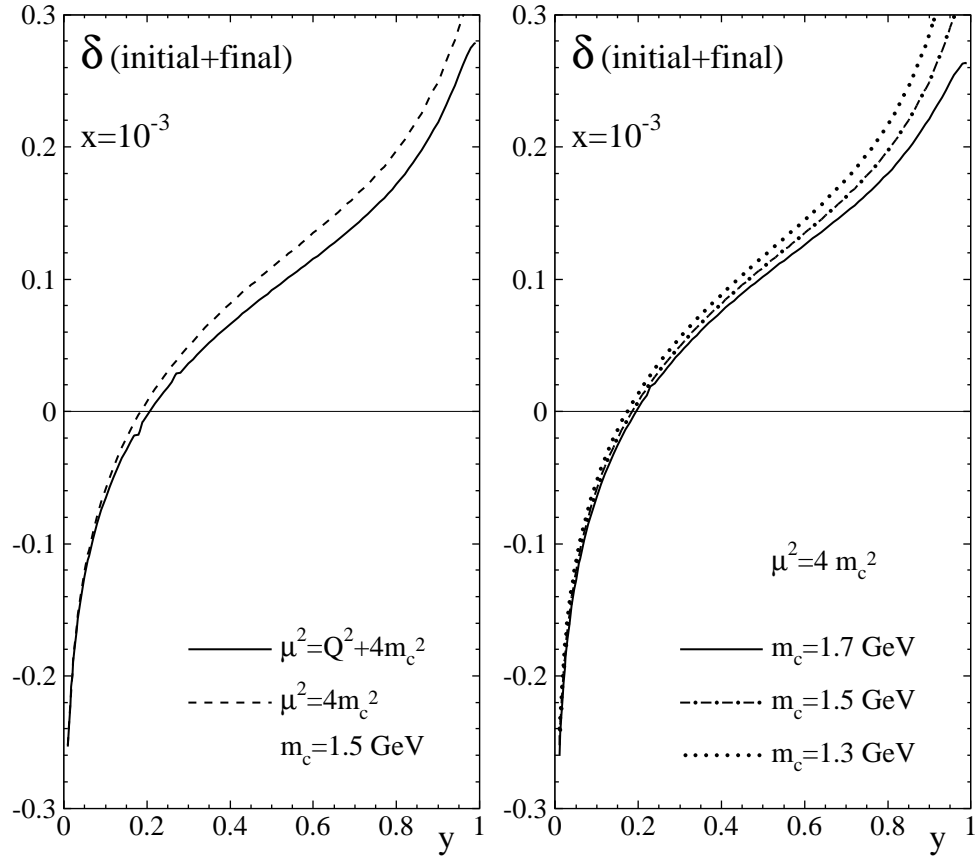


Figure 5: Left side: $\delta(x, y)$, for two different factorization scales $\mu^2 = Q^2 + 4m_c^2$ [3] (full line) and $\mu^2 = 4m_c^2$ [22] (dashed line) ($m_c = 1.5$ GeV). Right side: $\delta(x, y)$, using the charm masses $m_c = 1.3, 1.5, 1.7$ GeV ($\mu^2 = 4m_c^2$). (PDF: GRV94(LO) [21].)

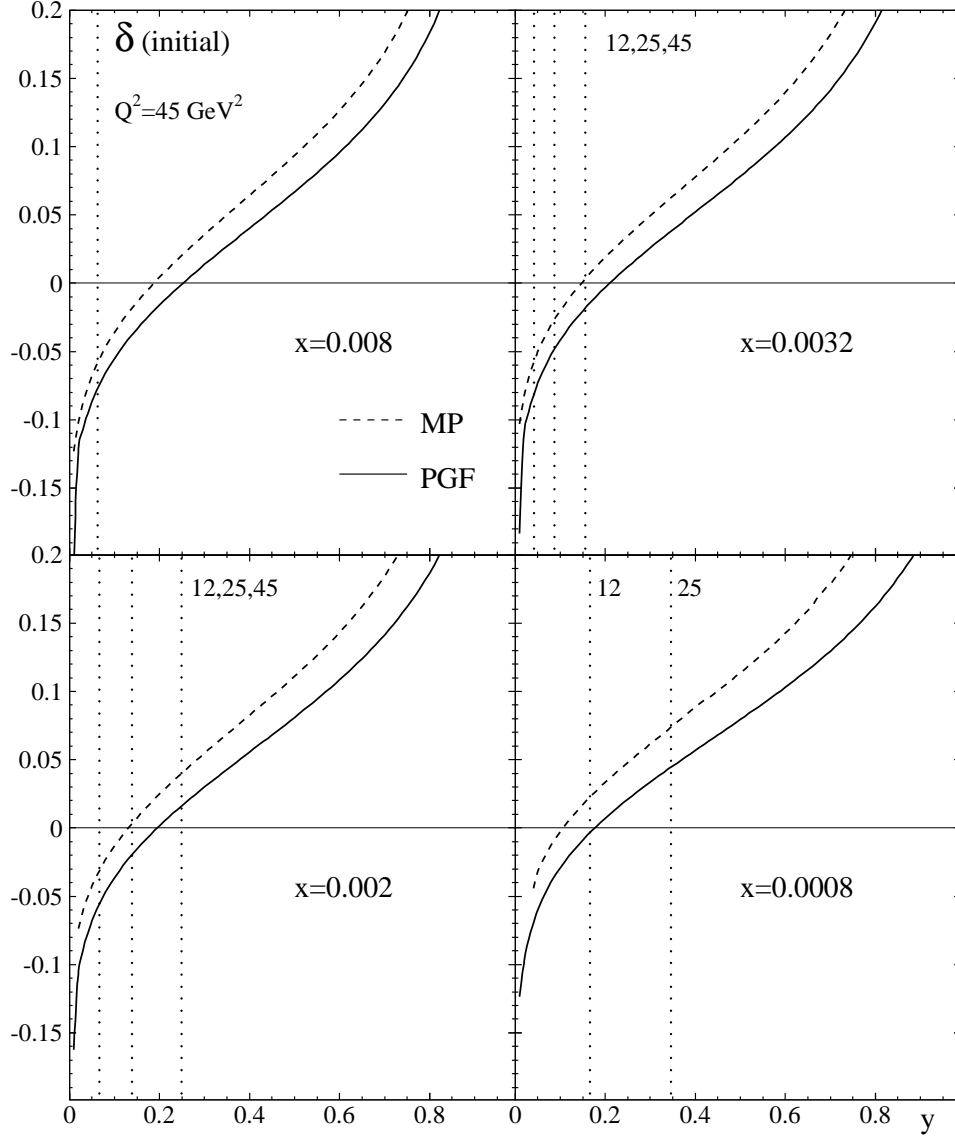


Figure 6: Comparison of massive (solid line, $\mu^2 = Q^2 + 4m_c^2$, $m_c = 1.5$ GeV) and massless (dashed line) radiative corrections δ (initial) for experimentally relevant x [1] using the parton distributions GRV92(LO) (MP) [23] and GRV94(LO) (PGF) [21]. The dotted vertical lines indicate values of constant $Q^2 = 12, 25$ or 45 GeV².

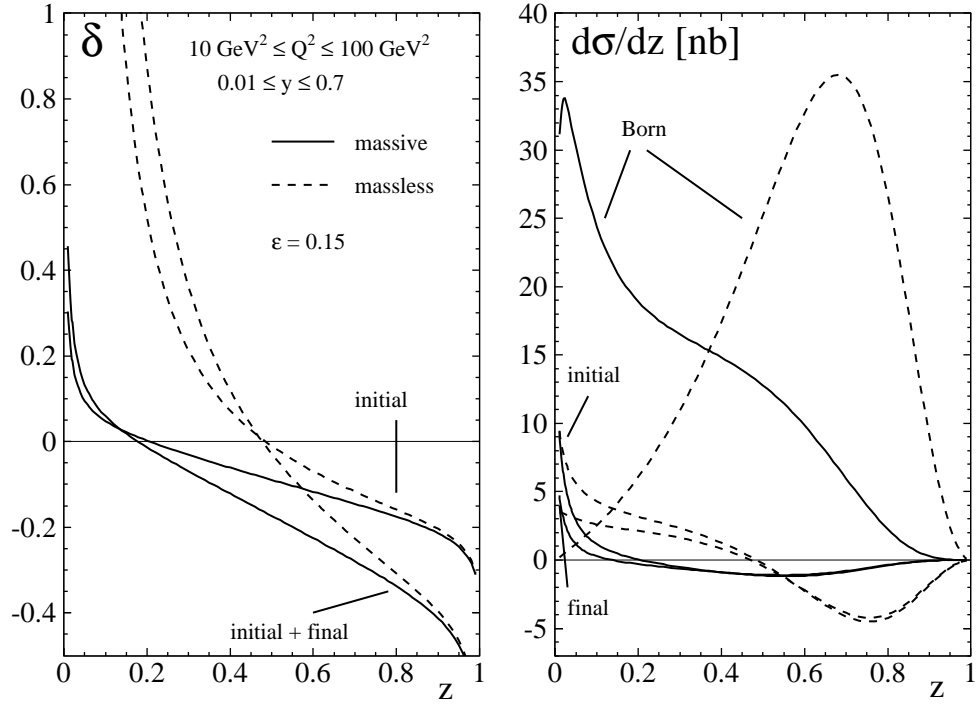


Figure 7: z -differential radiative corrections to massive ($m_c = 1.5$ GeV, $\mu^2 = Q^2 + 4m_c^2$) (full line) and massless (dashed) charm production, integrated over the kinematical range $10 \text{ GeV}^2 \leq Q^2 \leq 100 \text{ GeV}^2$, $0.01 \leq y \leq 0.7$, using the parton distributions GRV92(LO) (massless) [23] and GRV94(LO) (massive) [21] and a Peterson et al. fragmentation function [20] with $\varepsilon = 0.15$.

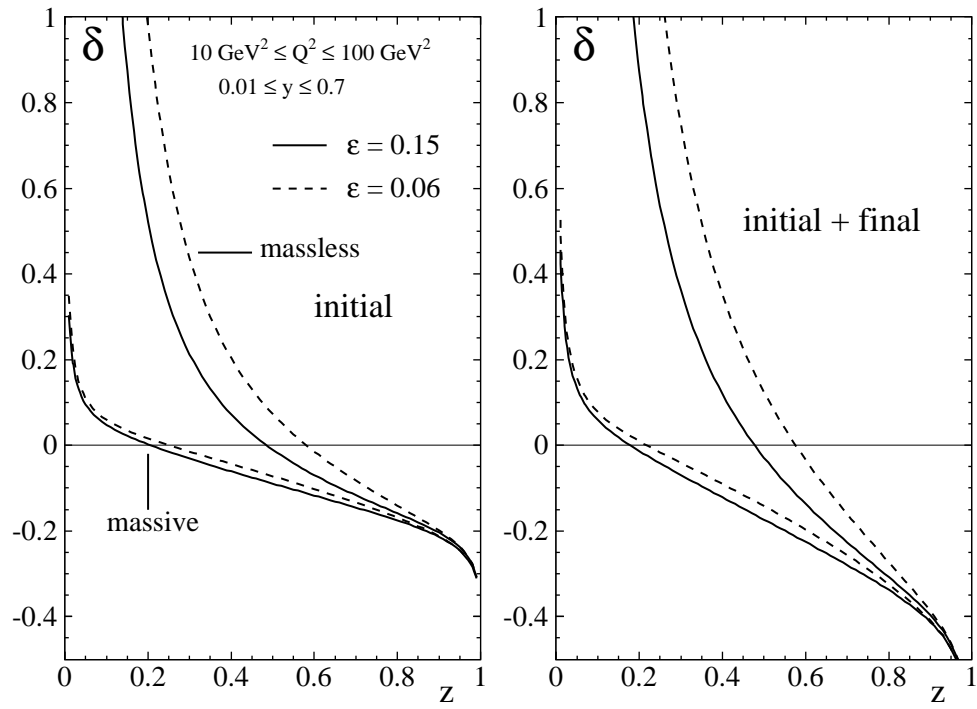


Figure 8: As fig. 7 (lhs) with $\epsilon = 0.15$ (full line) and $\epsilon = 0.06$ (dashed line). The contribution due to initial state radiation is shown (lhs) as well as the sum of initial and final state radiation (rhs).

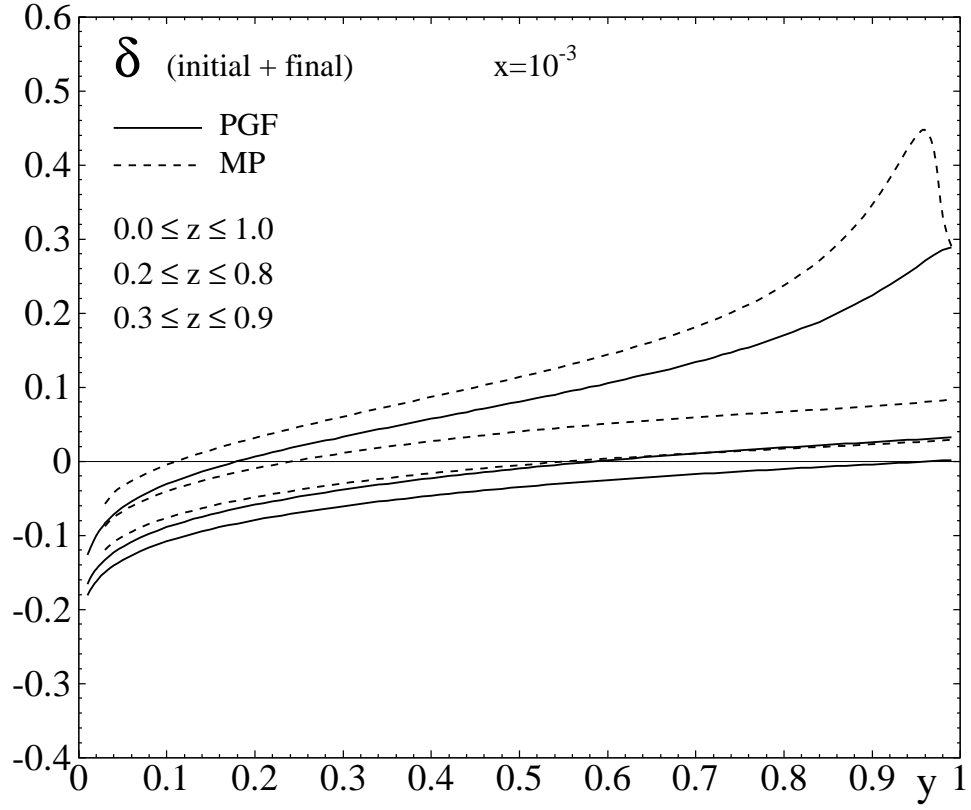


Figure 9: $\delta(x, y; z^{\min}, z^{\max})$ (defined in the text) in dependence of y for $x = 10^{-3}$ and three choices of z^{\min}, z^{\max} : From top to bottom $0 \leq z \leq 1$, $0.2 \leq z \leq 0.8$ and $0.3 \leq z \leq 0.9$. The massive corrections have been calculated employing the GRV94(LO) parton distributions [21] and the factorization scale $\mu^2 = Q^2 + 4m_c^2$ with $m_c = 1.5$ GeV. For the massless corrections we have taken the GRV92(LO) parton distributions [23]. In all cases we employed a Peterson et al. fragmentation function [20] with $\varepsilon = 0.15$.